Economic Modelling 28 (2011) 1106–1116

Contents lists available at ScienceDirect

Economic Modelling

journal homepage: www.elsevier.com/locate/ecmod

Modeling volatility with time-varying FIGARCH models

Mustapha Belkhouja *, Mohamed Boutahary [1]

GREQAM, Université de la Méditerranée, 2 rue de la Charité, 13002 Marseille, France

ARTICLE INFO

Article history:
Accepted 30 November 2010

JEL classification:
C12
C15
C22
C51
C52
G1
Q4

Keywords:
FIGARCH
Long memory
Nonlinear time series
Structural change
Time-varying parameter model

ABSTRACT

This paper puts the light on a new class of time-varying FIGARCH or *TV-FIGARCH* processes to model the volatility. This new model has the feature to account for the long memory and the structural change in the conditional variance process. The structural change is modeled by a logistic function allowing the intercept to vary over time. We also implement a modeling strategy for our *TV-FIGARCH* specification whose performance is examined by a Monte Carlo study. An empirical application to the crude oil price and the S&P 500 index is carried out to illustrate the usefulness of our techniques. The main result of this paper is that the long memory behavior of the absolute returns is not only explained by the existence of the long memory in the volatility but also by deterministic changes in the unconditional variance.

© 2010 Elsevier B.V. All rights reserved.

1. Introduction

The modeling of time-varying volatility has been a considerable field of research for a quarter of a century following the introduction of the Autoregressive Conditional Heteroskedasticity (*ARCH*) model by Engle (1982), then its extending to the Generalized *ARCH* (*GARCH*) model by Bollerslev (1986). It is a well known that many financial time series, whose sample autocorrelations are tiny, have sample autocorrelations of their absolute and squared values significantly different from zero even for large lags. This empirical finding is usually interpreted as evidence for long memory in the volatility of returns. Therefore, Baillie et al. (1996) and Bollerslev and Mikkelsen (1996) introduced long memory processes of the conditional variance by extending the *GARCH* model of Bollerslev (1986). The fractionally integrated long memory models have thus received considerable interest because of their ability to capture the persistence in the volatility. Additionally, it is also well known that the long memory is easily confused with structural changes, since the slow decay of the autocorrelation function, which is typical to a time series with long memory, is also produced when a short-memory time series exhibits structural breaks (Boes and Salas-La Cruz (1978), Hamilton and Susmel (1994), Diebold and Inoue (1999), Granger and Hyung (1999), Gourieroux and Jasiak (2001)). In this context, one may expect that economic and political events or changes in institutions are somehow responsible of changing in the volatility structure over time. Some explanations of the phenomenon have been suggested by Schwert (1989) among others, who relates alternating volatility regimes to the fluctuations in the fundamental uncertainty and leverage effects over the business cycle. Beltratti and Morana (2006) relate breaks in the stock market volatility to monetary policy reactions in response to business cycle conditions, while Engle and Rangel (2005), in addition to the macroeconomic uncertainty, and put the light on the market size and the development role. An intermediate position has suggested that an appropriate model for the volatility of financial returns should combine the long range dependence and the structural change (see Lobato and Savin (1998), Beran and Ocker (1999), Beine and Laurent (2000), Morana and Beltratti (2004), Martens et al. (2004), Baillie and Morana (2009)).

Given the above summary of previous research, the basic idea of this paper comes from the fact that the volatility of many financial returns is susceptible to the occurrence of both long memory and structural breaks. So, the purpose of this paper is twofold. The first is to introduce a model which allows for long memory and structural change in the time series volatility. The proposed model is named *time-varying FIGARCH*, or *TV-FIGARCH*, and augments the traditional *FIGARCH* model of Baillie, Bollerslev and Mikkelsen (1996) with a deterministic component following logistic functions. The suggested

* Corresponding author. Tel.: +33 6 42 10 09 18; fax: +33 4 91 90 02 27.
E-mail addresses: belkhouja_mustapha@yahoo.fr (M. Belkhouja), boutahar@lumimath.univ-mrs.fr (M. Boutahary).
[1] Tel.: +33 4 91 82 90 89; fax: +33 4 91 82 93 56.

0264-9993/$ – see front matter © 2010 Elsevier B.V. All rights reserved.
doi:10.1016/j.econmod.2010.11.017

parameterization describes structural changes in the baseline volatility where the transition between regimes over time may be smooth, depending on the slope parameter which controls the smoothness degree of shifts. A similar model named *Adaptive FIGARCH* has been proposes by Baillie and Morana (2009), expect that the intercept in the conditional variance equation is time varying according to the Gallant (1984) flexible functional form. Further, their approach does not use pre-testing for the number of transitions. The second aim of this paper is to give a modeling strategy for these new *TV-FIGARCH* models. In order to choose the right transition number, we implement a selection rule using the Lagrange multiplier method to test a sequence of hypotheses.

Finally, after parameter estimation, the model is evaluated by misspecification tests. Finite-sample properties of tests and estimations are examined by a simulation study; an empirical application to the daily crude oil price returns and the daily stock returns illustrates the usefulness and properties of our modeling strategy in practice. The empirical evidence favors the *TV-FIGARCH* formulation with two transition functions, indicating a clear rejection of the *FIGARCH* null hypothesis. The main result of this paper is that the long memory property of the absolute returns is explained both by structural changes in the unconditional variance and the presence of long memory in the volatility.

The outline of this paper is organized as follows. In Section 2, we present the class of *TV-FIGARCH* model and we discuss its properties. Section 3 considers the parameter constancy test by using a Lagrange Multiplier (LM) type test. In Section 4, we propose the specification strategy and the model estimation. Section 5 and 6 contain respectively the simulation study, using Monte Carlo experiments, and the empirical results. The last section concludes.

2. A time-varying FIGARCH Process

In this section we present the *time-varying FIGARCH*, or *TV-FIGARCH* process, which contains two basic components: the long memory in the volatility process and changes in the baseline volatility dynamics over time. We begin by introducing the *FIGARCH* (p, d, q) model following Baillie, Bollerslev and Mikkelsen (1996):

$$\begin{cases} \varepsilon_t = z_t\sqrt{h_t}, \quad \varepsilon_t\,|\,\Omega_{t-1} \sim N(0,h_t) \\ h_t = \omega_0 + \beta(L)h_t + \left[1-\beta(L)-[1-\phi(L)](1-L)^d\right]\varepsilon_t^2 \end{cases} \tag{1}$$

$\{z_t\}$ is a sequence of independent standard normal variables with variance 1, $\{h_t\}$ is a positive time dependent conditional variance defined as $h_t = E(\varepsilon_t^2|\Omega_{t-1})$ and Ω_{t-1} is the information set up to time *t-1*. Defining $\upsilon_t = \varepsilon_t^2 - h_t$ the *FIGARCH* (p, d, q) process may be rewritten as an *ARFIMA*(p, d, q):

$$[1-\phi(L)](1-L)^d\varepsilon_t^2 = \omega_0 + [1-\beta(L)]\upsilon_t \tag{2}$$

where $\beta(L) = \beta_1 L + ... + \beta_p L^p$ and $\phi(L) = \phi_1 L + ... + \phi_q L^q$. $[1-\beta(L)]$ and $[1-\phi(L)]$ have all their roots outside the unit circle. The fractional differencing operator $(1-L)^d$ with real d is defined by (Hosking (1981)):

$$(1-L)^d = \textstyle\sum_{k=0}^{\infty}\delta_k(d)L^k, \; \delta_k(d) = \dfrac{k-1-d}{k}\delta_{k-1}(d), \; \delta_0(d) = 1 \tag{3}$$

where L is the lag operator and d is the long memory parameter. We have a stationary long memory process when $0<d<1$. If $d=1$, the process has a unit root and thus a permanent shock effect.

An alternative representation of the *FIGARCH* (p, d, q) is the *ARCH* (∞) model:

$$\begin{aligned} h_t &= \frac{\omega_0}{[1-\beta(L)]} + \left[1-\frac{[1-\phi(L)](1-L)^d}{[1-\beta(L)]}\right]\varepsilon_t^2 \\ &= \frac{\omega_0}{[1-\beta(L)]} + \lambda(L)\varepsilon_t^2 \end{aligned} \tag{4}$$

where $\lambda(L) \equiv \lambda_1 L + \lambda_2 L^2 + ...$ and $\lambda(1) = 1$ for every d. The constraints applied to the parameters to guarantee the positivity of the conditional variance in (4) are: $\omega_0 > 0$ and $\lambda_i \geq 0$, for $i = 1, 2, ...$ The assumption of a constant intercept is not consistent if the baseline volatility dynamics change in the long run. For this purpose, we extend the *FIGARCH*(p, d, q) to the *TV-FIGARCH*(p, d, q, R) process, which allows the intercept to be time dependent. The *TV-FIGARCH* model has the feature to be flexible enough to explain the systematic movements of the baseline volatility. Hence, the model in (1) becomes:

$$\begin{cases} \varepsilon_t = z_t\sqrt{h_t}, \quad \varepsilon_t\,|\,\Omega_{t-1} \sim N(0,h_t) \\ h_t = \omega_0 + \beta(L)h_t + \left[1-\beta(L)-[1-\phi(L)](1-L)^d\right]\varepsilon_t^2 + f_t \end{cases} \tag{5}$$

$$f_t = \sum_{r=1}^{R}\omega_r F_r(s_t,\gamma_r,c_r) \tag{6}$$

where $F(s_t,\gamma_r,c_r)$, $r = 1,..,R$, are the transition functions governing the switches from one regime to another. These functions are continuous, non-negative and bounded between zero and one allowing the intercept of the *FIGARCH* model to fluctuate over time between ω_0 and $\omega_0 + \sum_{r=1}^{R}\omega_r$. The order $R \in \mathbb{N}$ determines the shape of the baseline volatility. A suitable choice for $F(s_t,\gamma_r,c_r)$, $r = 1,..,R$, is the general logistic transition function defined as follows:

$$F_r(s_t,\gamma_r,c_r) = (1 + exp\{-\gamma_r(s_t-c_r)\})^{-1} \tag{7}$$

with the slope parameter γ_r ($\gamma_r > 0$) which controls the degree of smoothness. c_r is the threshold parameter such as $c_1 \leq c_2 \leq ... \leq c_R$. $s_t = t/T$ is the transition variable and T is the number of observations. When $\gamma_r \to \infty$, the switch from one state to another is abrupt, that is, a smooth change approaches a structural break at the threshold parameter c_r.

Eventually, the *TV-FIGARCH* (p, d, q) process will not be ergodic and nor strictly stationary, due to the time varying intercept. Because the *FIGARCH* (1,d,1) model is the most frequently used specification in empirical applications, we focus on the conditions that guarantee the non negativity of its conditional variance and we follow the restrictions proposed recently by Conrad and Haag (2006), i.e.:

$\omega_0 > 0$
If $0 < \beta_1 < 1$;
either $\lambda_1 \geq 0$ and $\phi_1 \leq f_2$ or for $i > 2$ with $f_{i-1} < \phi_1 \leq f_i$ it holds that $\lambda_{i-1} \geq 0$.
If $-1 < \beta_1 < 0$;
either $\lambda_1 \geq 0$, $\lambda_2 \geq 0$ and $\phi_1 \leq f_2(\beta_1+f_3)/(\beta_1+f_2)$ or for $i > 3$ with $f_{i-2}(\beta_1+f_{i-1})/(\beta_1+f_{i-2}) < \phi_1 \leq f_{i-1}(\beta_1+f_i)/(\beta_1+f_{i-1})$ it holds that $\lambda_{i-1} \geq 0$ and $\lambda_{i-2} \geq 0$.

Note, that $\lambda_0 = 1$, $\lambda_1 = d + \phi_1 - \beta_1$, $\lambda_i = \beta\lambda_{i-1} + (f_i - \phi_1)(-g_{i-1})$ for $i > 1$, $f_j = (j-1-d)/j$, for $j = 1,2,...$ and $g_j = f_j.g_{j-1}$. So, for the *FIGARCH*(1,d,1) model it suffices to check 2 conditions if $0 < \beta_1 < 1$ and 3 conditions if $-1 < \beta_1 < 0$ to ensure the non-negativity of the conditional variance for all t. Similar restrictions, ensuring the positivity of h_t, hold for the *TV-FIGARCH*(1,d,1) model in addition to the restriction $\omega_0 + \sum_{r=1}^{R} \omega_r > 0$. The *TV-FIGARCH*(1,d,1) nests two interesting submodels: the *TV-FIGARCH* (1,d,0) and the *TV-FIGARCH*(0, d,1) whose restrictions ensuring the positivity of h_t are similar to those holding for the *FIGARCH* (1,d,0) and the *FIGARCH*(0,d,1) models in addition to the restriction $\omega_0 + \sum_{r=1}^{R} \omega_r > 0$[2].

3. Testing parameter constancy

This test has previously been considered by Lundbergh and Teräsvirta (2002) and Teräsvirta and Amado (2008) for the *GARCH* model, but for our purpose we will apply it to the *FIGARCH* model in order to check wether the intercept is time dependent. We test the *TV-FIGARCH* with one transition function and if the intercept constancy hypothesis is rejected, one may conclude that fitting a *FIGARCH* model to the data does not seem reasonable. In order to derive the test statistic let us rewrite the model (5) with one transition function i.e.:

$$\begin{cases} \varepsilon_t = z_t\sqrt{h_t}, \quad \varepsilon_t|\Omega_{t-1}\sim N(0,h_t) \\ h_t = \omega_0 + \beta(L)h_t + \left[1-\beta(L)-[1-\phi(L)](1-L)^d\right]\varepsilon_t^2 + \omega_1 F_1(s_t,\gamma_1,c_1) \end{cases} \tag{8}$$

The null hypothesis of the test corresponds to $H_0:\gamma_1=0$ against $H_1:\gamma_1>0$, but under the null hypothesis ω_1 and c_1 are not identified. This identification problem has been resolved by Luukkonen et al. (1988) by replacing the transition function by its first order Taylor approximation around $\gamma_1=0$ [3]. The first order Taylor expansion of the logistic transition function around $\gamma_1=0$ is given by:

$$T_1(s_t,\gamma_1,c_1) = \frac{1}{4}\gamma_1(s_t-c_1) + R(s_t,\gamma_1,c_1) \tag{9}$$

where $R(s_t,\gamma_1,c_1)$ is a remainder term. Replacing $F_1(s_t,\gamma_1,c_1)$ in (8) by $T_1(s_t,\gamma_1,c_1)$ in (9) and after rearranging terms we have:

$$\begin{cases} \varepsilon_t = z_t\sqrt{h_t}, \quad \varepsilon_t|\Omega_{t-1}\sim N(0,h_t) \\ h_t = \omega_0^* + \beta(L)h_t + \left[1-\beta(L)-[1-\phi(L)](1-L)^d\right]\varepsilon_t^2 + \omega_1^* s_t + R(s_t,\gamma_1,c_1) \end{cases} \tag{10}$$

where $\omega_0^* = \omega_0 - \frac{1}{4}\omega_1\gamma_1$, $\omega_1^* = \frac{1}{4}\gamma_1\omega_1$, therefore, the null hypothesis for parameter constancy becomes: $H_0:\omega_1^*=0$. Under H_0, the remainder $R=0$, so it does not affect the asymptotic null distribution of the test statistic.

Let $\theta=(d,\omega_0^*,\beta',\phi',\omega_1^*)'$, the partial derivatives evaluated under H_0 are given by:

$$\left.\frac{\partial l_t}{\partial\theta}\right|_{H_0} = \frac{1}{2}\left(\frac{\hat{\varepsilon}_t^2}{\hat{h}_{0t}}-1\right)\left.\frac{\partial \ln h_t}{\partial\theta}\right|_{H_0} \tag{11}$$

- $$\left.\frac{\partial \ln h_t}{\partial d}\right|_{H_0} = \left(\hat{h}_{0t}\right)^{-1}\left(-\ln(1-L)\left[1-\hat{\phi}(L)\right](1-L)^d\hat{\varepsilon}_t^2 + \sum_{j=1}^{p}\hat{\beta}_j\frac{\partial\hat{h}_{t-j}}{\partial d}\right)$$
$$= \left(\hat{h}_{0t}\right)^{-1}\left(-\left[1-\hat{\phi}(L)\right](1-L)^d\sum_{j}^{t-1}\frac{\hat{\varepsilon}_{t-j}^2}{j} + \sum_{j=1}^{p}\hat{\beta}_j\frac{\partial\hat{h}_{t-j}}{\partial d}\right)$$
- $$\left.\frac{\partial \ln h_t}{\partial\omega_0^*}\right|_{H_0} = \left(\hat{h}_{0t}\right)^{-1}\left(1 + \sum_{j=1}^{p}\hat{\beta}_j\frac{\partial\hat{h}_{t-j}}{\partial\omega_0^*}\right)$$
- $$\left.\frac{\partial \ln h_t}{\partial\beta}\right|_{H_0} = \left(\hat{h}_{0t}\right)^{-1}\left((h_{t-1},\ldots,h_{t-p})' - \left(\varepsilon_{t-1}^2,\ldots,\varepsilon_{t-p}^2\right)' + \sum_{j=1}^{p}\hat{\beta}_j\frac{\partial\hat{h}_{t-j}}{\partial\beta}\right)$$
- $$\left.\frac{\partial \ln h_t}{\partial\phi}\right|_{H_0} = \left(\hat{h}_{0t}\right)^{-1}\left((1-L)^{\hat{d}}\left(\varepsilon_{t-1}^2,\ldots,\varepsilon_{t-q}^2\right)' + \sum_{j=1}^{p}\hat{\beta}_j\frac{\partial\hat{h}_{t-j}}{\partial\phi}\right)$$
- $$\left.\frac{\partial \ln h_t}{\partial\omega_1^*}\right|_{H_0} = \left(\hat{h}_{0t}\right)^{-1}\left(s_t + \sum_{j=1}^{p}\hat{\beta}_j\frac{\partial\hat{h}_{t-j}}{\partial\omega_1^*}\right)$$

Under the null hypothesis, the "hats" indicate the maximum likelihood estimators and $\hat{h}_{0t}$ denotes the conditional variance estimated at time t. The LM-type statistic is asymptotically distributed under H_0 as χ^2 with one degree of freedom:

$$LM = \frac{1}{2}\sum_{t=1}^{T}\hat{u}_t\hat{X}_t'\left(\sum_{t=1}^{T}\hat{X}_t\hat{X}_t'\right)^{-1}\sum_{t=1}^{T}\hat{u}_t\hat{X}_t \tag{12}$$

where $\hat{u}_t = \left(\frac{\hat{\varepsilon}_t^2}{\hat{h}_{0t}}-1\right)$ and $\hat{X}_t = \left.\frac{\partial \ln h_t}{\partial\theta}\right|_{H_0}$.

In practice this test may be carried out in a straightforward way using an auxiliary least squares regression, thus:

- Firstly, estimate consistently the parameters of the conditional variance under the null hypothesis, compute the residuals $\hat{u}_t = \left(\frac{\hat{\varepsilon}_t^2}{\hat{h}_{0t}}-1\right)$, $t=1,\ldots,T$, then the sum of squared residuals $SSR_0 = \sum_{t=1}^{T}\hat{u}_t^2$.
- Secondly, regress $\hat{u}_t$ on $\hat{X}_t'$, $t=1,\ldots,T$, and compute the sum of squared residuals, SSR_1.
- Finally, compute the χ^2 test statistic by:

$$LM = \frac{T(SSR_0-SSR_1)}{SSR_0} \tag{13}$$

4. Specification and estimation of the model

In order to build the *TV-FIGARCH* model in (5), we start with a simple and restricted specification without time-varying parameters. Our modeling strategy contains the following stages:

- The first step is to filter the short memory from the series by using a simple *ARMA* model and obtain the residuals $\hat{\varepsilon}_t$.
- We check the presence of long memory in the volatility using the autocorrelation functions (ACF) of the squared residuals $\hat{\varepsilon}_t^2$, and then we select a parsimonious *FIGARCH* model. In practice a *FIGARCH*(1,d,1) specification is sufficient. The squared standardized errors should be free of serial correlation because neglected autocorrelations may bias the test of parameter constancy.
- The next stage consists on choosing the number of transitions. We use a selection rule based on a sequence of LM-type tests. We assume that $Rmax=5$ for more flexibility of the transition function f_t in (6). Thus, we have five hypotheses to test:

$H_{05}:\omega_5^*=0,$
$H_{04}:\omega_4^*=0|\ \omega_5^*=0,$
$H_{03}:\omega_3^*=0|\ \omega_4^*=\omega_5^*=0,$

[2] For more details on the nonegativity of the FIGARCH(1,d,0) and the FIGARCH(0,d,1) models see Conrad and Haag (2006).

[3] For the purpose of deriving the test, we replace $F_1(s_t,\gamma_1,c_1)$ by $F_1(s_t,\gamma_1,c_1)-1/2$, (See Teräsvirta and Amado (2008)).

$H_{02}:\omega_2^*=0|\ \omega_3^*=\omega_4^*=\omega_5^*=0,$
$H_{01}:\omega_1^*=0|\ \omega_2^*=\omega_3^*=\omega_4^*=\omega_5^*=0,$
of course the selected order R corresponds to the lowest p-value among those of the rejected null hypothesis. If any null hypothesis is rejected, therefore, there is no structural change in the volatility.

- Despite the non stationarity of the *ARMA-TV-FIGARCH* process due to the time varying baseline volatility, we use the quasi maximum likelihood method to estimate the selected model, and then we evaluate it by some diagnostic tests. Note that this method is valid in non standard frameworks[4].

Let $\lambda=(\mu,\pi',\psi',d,\omega_0,\beta',\phi',\omega',\gamma',c')'$ where $\mu,\pi'=(\pi_1,...,\pi_i)$ and $\psi'=(\psi_1,...,\psi_j)$ are the *ARMA* parameters, and $\beta=(\beta_1,..,\beta_p)'$, $\phi=(\phi_1,..,\phi_q)'$, $\omega=(\omega_0,\omega_1,..,\omega_R)'$, $\gamma=(\gamma_1,..,\gamma_R)'$ and $c=(c_1,..,c_R)'$ are the *TV-FIGARCH* parameters. The quasi maximum likelihood estimate of the parameter vector λ is obtained by:

$$\hat{\lambda}=arg\max_{\lambda\in\Lambda}\frac{1}{T}\sum_{t=1}^{T} l_t(\lambda) \tag{14}$$

where $l_t(\lambda)$ is the quasi log-likelihood of the model for observation t :

$$l_t(\lambda)=-\frac{1}{2}ln2\pi-\frac{1}{2}lnh_t-\frac{1}{2}\frac{\varepsilon_t^2}{h_t} \tag{15}$$

Under fairly general conditions, the asymptotic distribution of the *QMLE* is

$$T^{1/2}\left(\hat{\lambda}-\lambda_0\right)\overset{A}{\sim}N\left\{0,A(\lambda_0)^{-1}B(\lambda_0)A(\lambda_0)^{-1}\right\} \tag{16}$$

where λ_0 denotes the true vector of parameters, $A(\lambda_0)$ is the Hessian and $B(\lambda_0)$ the outer product gradient. The proposed method allows to jointly estimate long memory and structural changes in the conditional variance. We note that large estimates for the smoothness parameter γ_r may lead to numerical problems when testing the parameter constancy. As solution to this problem, Eitrheim and Terasvirta (1996) suggested to omit score elements that are partial derivatives with respect to the parameters of the transition function $F_r(s_t,\gamma_r,c_r)$.

5. Simulation study

5.1. Monte Carlo design

In all simulations, we use sample lengths of 1000, 2000 and 3000 observations and, for each design, a total of 100 replications were generated. To avoid the initialization effects, a total of 7000 observations were discarded from each replication. In the simulations and the estimation results we fixed the truncation lag at $j=1000$[5]. The behavior of the tests is examined for several data generating processes (DGP's) that can be nested in the model in (5) with $p=1$ and $q=1$. The transition variable is the standardized time variable $s_t=t/T$, for $t=1...T$ and T is the number of observations. The data generating processes are as followings:

- DGP (I)

$$\varepsilon_t=z_t\sqrt{h_t},\quad \varepsilon_t|\Omega_{t-1}\sim N(0,h_t)$$
$$h_t=\omega_0+\beta h_{t-1}+\left[1-\beta L-[1-\phi L](1-L)^d\right]\varepsilon_t^2$$
$$d=\{0.25,0.50,0.75\},\omega_0=0.50,\beta=\{0.20,0.30,0.60\},\phi=\{0.20,0.30,0.60\}.$$

- DGP (II)

$$\varepsilon_t=z_t\sqrt{h_t},\quad \varepsilon_t|\Omega_{t-1}\sim N(0,h_t)$$
$$h_t=\omega_0+\beta h_{t-1}+\left[1-\beta L-[1-\phi L](1-L)^d\right]\varepsilon_t^2+\omega_1F_1(s_t,\gamma_1,c_1)$$
$$d=\{0.25,0.50,0.75\},\omega_0=0.50,\beta=\{0.20,0.30,0.60\},\phi=\{0.20,0.30,0.60\}$$
$$\omega_1=-0.30,\gamma_1=10, and\, c_1=0.5.$$

- DGP (III)

$$\varepsilon_t=z_t\sqrt{h_t},\quad \varepsilon_t|\Omega_{t-1}\sim N(0,h_t)$$
$$h_t=\omega_0+\beta h_{t-1}+\left[1-\beta L-[1-\phi L](1-L)^d\right]\varepsilon_t^2+\omega_1F_1(s_t,\gamma_1,c_1)+\omega_2F_2(s_t,\gamma_2,c_2)$$
$$d=\{0.25,0.50,0.75\},\omega_0=0.50,\beta=\{0.20,0.30,0.60\},\phi=\{0.20,0.30,0.60\}$$
$$\omega_1=-0.30,\omega_2=0.30,\gamma_1=10,\gamma_2=10,c_1=0.3\, and\, c_2=0.7.$$

Figs. 1 and 2 show the plots of the series, the autocorrelation absolute series function, the transition function f_t and the conditional standard deviations respectively for DGP(II) and DGP(III) with $T=2000$, $d=0.25$, $\beta=0.20$ and $\phi=0.60$. The absolute series autocorrelation functions exhibit persistence due to the presence of both long memory and structural changes in the two DGP's. Moreover, we notice in Fig. 1 a decrease of the conditional standard deviation while in Fig. 2, it decreases at first, then increases. These two phenomena are explained by the variation of the *FIGARCH* intercept according to the transition function f_t where the switch from one parameterization to another is smooth.

5.2. Size and power simulations

In this section, we study the size and the power properties of the LM-type test using the Monte Carlo simulation method. Tests are computed using auxiliary regressions. The size and the power results of the tests are presented in Tables 1 and 2 and for each test we calculate the rejection frequency for three sample sizes at the following nominal levels: 1%, 5% and 10%. The size results in Table 1 have been obtained by generating the artificial data from the DGP (I). We notice that the estimated sizes are away from nominal levels when the parameter of long memory d increases but the results become more accurate as the sample size rises. Generally the tests are reasonably well-sized.

The power results in Table 2 have been obtained by generating the artificial data from the DGP (II) where $\omega_1=-0.30$, $\gamma_1=10$ and $c_1=0.50$. The rejection frequencies show some distortions when $T=1000$ and $d\geq0.5$. As expected, the rejection frequencies are an increasing function of the sample size, however, the results are less accurate as the parameter of long memory d increases. We can explain the underestimation of the rejection frequencies by the likely confusion between long memory and regime changes, i.e. the structural change in the volatility may be partially captured by the long memory component of the *FIGARCH* process. Teräsvirta and Amado (2008) conduct similar simulation experiments to evaluate the finite-sample properties of the parameter constancy tests, but these tests are against an additive and a multiplicative time-varying GARCH specifications. Their findings suggest that the parameter constancy tests have reasonable good properties for moderate samples.

5.3. Model selection simulations

In this section we consider the performance of the modeling strategy for *TV-FIGARCH* models. Again, for each DGP a total of 100 replications were carried out for every sample size and the results of the test are shown at 5% nominal significance level. The selection procedure of the transitions number was employed until a maximum of $R=2$, so we have two hypothesis to test at each experience using the LM-type test. The selected number of transitions corresponds to the rejected null hypothesis providing the less p-value. If any null hypothesis is rejected R will be equal to zero and the selected model is *FIGARCH*. We begin by considering a standard *FIGARCH* model as a DGP and its selection frequencies are reported in Table 3. The frequencies of the correct number of transitions are shown in bold face. We notice that the selection of the correct model becomes less frequent as the long memory parameter d converges to one, in the other hand, the results become more accurate as the sample size increases. The frequencies of selecting the models for the DGP (II) are presented in Table 4. As for the DGP (I), the sample size and the long memory parameters have the

[4] see queryDahlhaus and Subba Rao (2006).
[5] See Baillie, Bollerslev and Mikkelsen (1996).

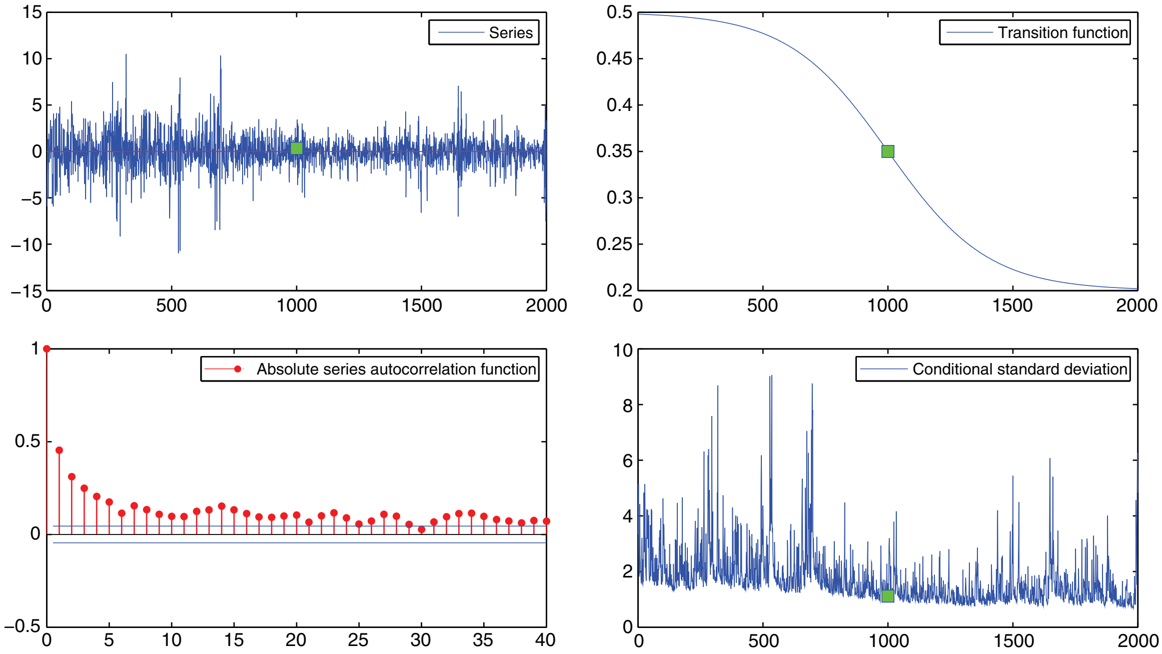

Fig. 1. Plots of the series, the autocorrelation absolute series function, the transition function f_t and the conditional standard deviations with $R = 1$.

same effects on the accuracy of the results. Table 5 contains the frequencies of the selected models for the DGP (III) and the results are almost identical to what is reported in Table 3 and Table 4. As expected, the correct model is selected more frequently for higher sample size and the selection procedure seems to work relatively well besides the bad impact of the long memory parameter increase on the results accuracy. We notice that the power of the procedure was not affected by the number of transitions in the volatility.

5.4. Estimation results

This section reports some simulation results from estimating *TV-FIGARCH* models with different levels of long memory and under various forms of structural change. The length of the simulated time series is equal to 3000 observations. Tables 6 through 8 report the true values of parameters and the mean of their estimates across 100 Monte Carlo replications. The data are generated from the *FIGARCH*(1,d,1), the *TV-FIGARCH*(1,d,1,1) and the *TV-FIGARCH*(1,d,1,2) models. The root mean square error (RMSE) are relatively high when $d = 0.50$ and ω_2 seems to have better performance than ω_1 that may be explained by the negative sign of the latter. The bias of c_1 and c_2 appears to noticeably decrease as the long memory parameter increases but that has no effect on their RMSE. The slope parameters γ_1 and γ_2 have the worst estimation results compared to the rest of parameters. Note that the mean of the QMLE standard error (SE) are generally close to the root mean square error (RMSE). The approximate maximum likelihood method for the *FIGARCH*

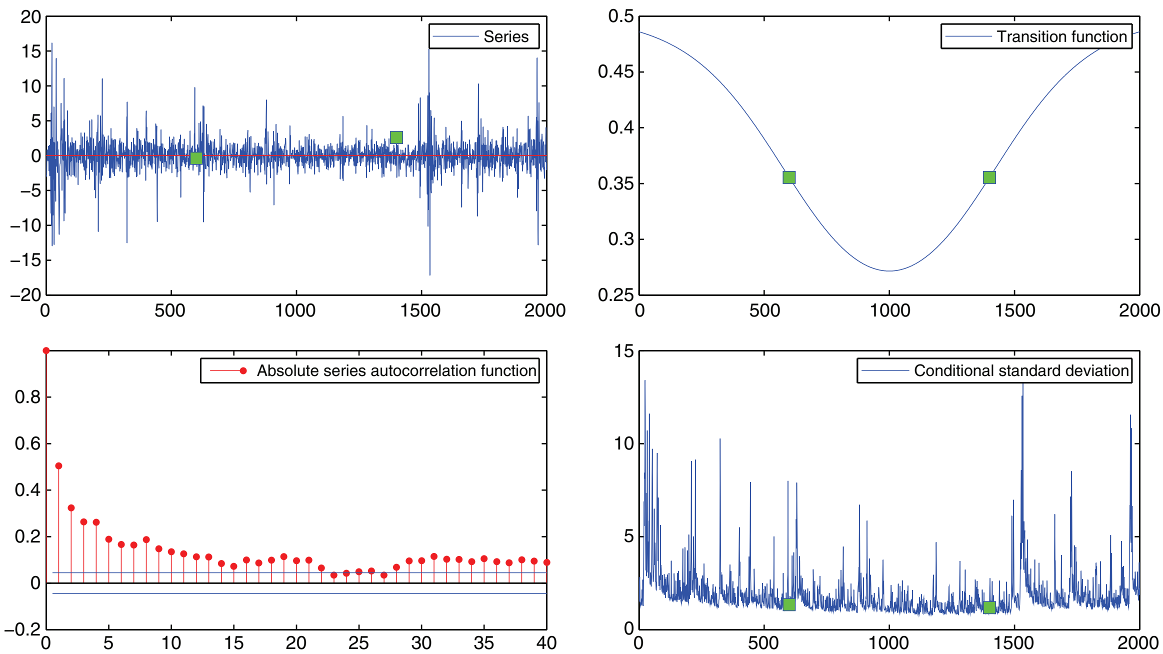

Fig. 2. Plots of the series, the autocorrelation absolute series function, the transition function f_t and the conditional standard deviations with $R = 2$.

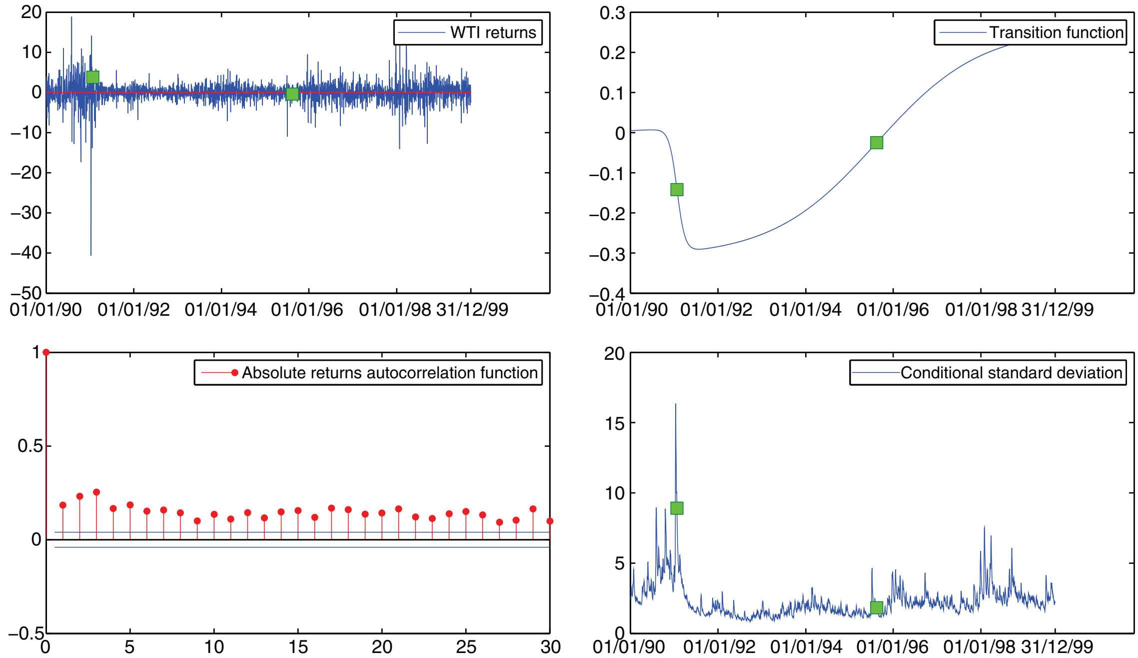

Fig. 3. Plots of the WTI returns, the absolute returns autocorrelation function, the transition function f_t and the conditional standard deviations.

and *TV-FIGARCH* models works reasonably well especially for the long parameter *d* which is very important in the sense that the persistence caused by the structural change won't be captured by the long memory component of the model.

6. Applications

This section presents two empirical examples involving the daily crude oil spot price (Dollars per Barrel) of West Texas Intermediate (WTI), which is used as a benchmark in oil pricing and the Standard and Poor 500 composite index (S&P 500). Both data series were from January 2, 1990 to December 31, 1999 and were taken from the Yahoo-Quotes database. All days the markets were closed and were removed, with the number of days removed varying between seven and nine depending on the year. After removing these days there were 2530 observations for the sample. Both series are transformed into the continuously compounded rates of returns, because it's known that the prices are non stationary in level but stationary in difference. We test the null hypothesis of non-stationary returns using the Augmented Said and Dickey (1984), the Phillips and Perron (1988) and the Kwiatkowski et al. (1992) tests. We employ the Akaike information criteria (AIC) to select the appropriate lag length[6]. Table 9 reports the test statistics where the regression is with only an intercept and with an intercept and a trend. The results clearly show that the WTI and S&P 500 returns are stationary at the 1% level. An *AR(3)* model is adapted for both returns to filter the short memory in the conditional mean.

6.1. WTI returns

The Table 10 shows that the WTI returns is more volatile than the S&P 500 returns with a standard deviation equals to 2.52. In terms of average returns, we do not notice a big difference between the two series over the sample period. The distribution of the WTI returns is negatively skewed and characterized by a statistically kurtosis suggesting that the underlying series is leptokurtic. Based on the high Jaque-Bera statistic, the marginal distribution of the WTI returns is far from normal. The Ljung-Box test applied to the returns and squared returns, provides clear evidence against the hypothesis of serial independence of observations, and as expected, the null hypothesis of no ARCH effect is strongly rejected. From the plot of the WTI returns (see Fig. 3) we observe two periods of large volatility in the beginning and at the second half of the sample, whereas we notice a decrease of volatility in the intermediate regime. The ACF of the absolute returns exhibits an extremely slow decaying pattern characterizing a long memory behavior in the volatility. Table 11 contains the LM test statistics and the p-values corresponding to the tested hypothesis as explained in section 4. The selection procedure of the transitions number was employed until a maximum of $R = 5$, so we have five hypothesis to test. The parameter constancy hypothesis is rejected for H_{02}, H_{03} and H_{04}, but we select $R = 2$ since it corresponds to the lowest p-value. This finding is not at all surprising because previous empirical studies indicate that commodity prices can be extremely volatile at times, and sudden changes in volatility are quite common in commodity markets. For example, using an iterative cumulative sum-of-squares approach, Wilson et al. (1996) document sudden changes in the unconditional variance in daily returns on one-month through six-month oil futures and relate these changes to exogenous shocks, such as unusual weather, political conflicts and changes in OPEC oil policies. Fong and See (2002) conclude that regime switching models provide a useful framework for studying factors behind the evolution of volatility and short-term volatility forecasts.

For the WTI returns, the estimate of the deterministic component f_t, presented in (6), has the following form:

$$f_t = \{1.37 - 1.31F_1(s_t, \hat{\gamma}_1, \hat{c}_1) + 0.57F_2(s_t, \hat{\gamma}_2, \hat{c}_2)\}$$

with

$$F_1(s_t, \hat{\gamma}_1, \hat{c}_1) = (1 + exp\{-106.14(s_t - 0.11)\})^{-1}$$

and

$$F_2(s_t, \hat{\gamma}_2, \hat{c}_2) = (1 + exp\{-8.15(s_t - 0.58)\})^{-1}$$

The graph of the transition function f_t (see Fig. 3) shows how volatility at first decreases abruptly ($\hat{\gamma}_1 = 106.14$), and then

[6] We assume the maximum given lags to be 24.

increases smoothly ($\hat{\gamma}_2 = 8.15$) over time. The first break in volatility ($\hat{c}_1 = 0.11$) is somewhat related to the economic and the political events happened in the 1990s. During this period, the crude oil prices are relatively low and oscillate between 10 and 20 dollars the barrel. The first high volatility of oil price returns corresponds to the launching of the Gulf War (1990–1991) which causes a sharp rise in the oil prices, then a return to the initial equilibrium. The second break in volatility ($\hat{c}_2 = 0.58$) is in line with the economic boom in the United States and Asia in the mid-1990s followed by the financial crisis of the latter. This crisis puts an end to the sharp upturn in oil prices from 1997 until February 1999. The long memory parameter estimate ($\hat{d} = 0.57$) indicates a high persistence in the volatility. This finding attests for the real presence of long memory in the volatility in addition to the nonlinearity caused by the change of the intercept over time according to the transition function. An *AR*(3)-*TV-FIGARCH*(1, d,1,2) is thus tentatively accepted as our final model for the WTI returns and The QML estimates are reported in Table 12. From Table 13 it is seen that there is neither serial correlation nor remaining ARCH in the standardized errors and thus the model seems to be adequately specified. The kurtosis coefficient has decreased substantially from its original value, but it is still high, and the skewness has been reduced from -1.63 to -0.27, but it remains negative. The hypothesis of normality is still strongly rejected.

6.2. S&P 500 returns

The summary statistics for the S&P 500 returns are given also by the Table 10 and show that the distributions of the series are skewed to the left with heavy tails. The Jarque-Bera test is in line with this evidence since it strongly rejects normality for the distribution of the S&P 500 returns. The Ljung-Box test applied to the returns and squared returns, provides clear evidence against the hypothesis of serial independence of observations and indicates the existence of ARCH effect which is confirmed by the ARCH test. At first sight to the Fig. 4, it appears that the dynamics of the S&P 500 volatility is similar to that of the WTI volatility with three regimes. In the same figure we find the plot of the sample autocorrelation of the absolute daily returns and we notice a persistence in the volatility. The results of the parameter constancy tests show that the null hypothesis is rejected for H_{02} and H_{05}, however a model with two transitions is accepted as the final model since it corresponds to the lowest p-value (see Table 11). This finding is consistent with the evidence of the presence of structural breaks in the S&P500 returns, previously detected by Lobato and Savin (1998), Granger and Hyung (2004), Starica and Granger (2004), Beltratti and Morana (2006), Baillie and Morana (2009). For the S&P 500 returns, the estimate of the transition function f_t has the following form:

$$f_t = \{0.45 - 0.39F_1(s_t,\hat{\gamma}_1,\hat{c}_1) + 0.33F_2(s_t,\hat{\gamma}_2,\hat{c}_2)\}$$

with

$$F_1(s_t,\hat{\gamma}_1,\hat{c}_1) = (1 + exp\{-24.67(s_t - 0.15)\})^{-1}$$

and

$$F_2(s_t,\hat{\gamma}_2,\hat{c}_2) = (1 + exp\{-24.97(s_t - 0.68)\})^{-1}$$

The graph of the deterministic component is depicted in Fig. 4 and looks like the one of the WTI volatility, i.e. firstly decreases then increases. However, the transition from the first regime to the second is smoother since the associated smoothness parameter ($\hat{\gamma}_1 = 24.67$) is clearly lower. We notice that the estimated threshold parameters ($\hat{c}_1 = 0.15$ and $\hat{c}_2 = 0.68$) are slightly higher than those of the WTI transition functions. From this empirical finding, we can deduce that the instability of the S&P 500 volatility is probably due to the same events presented above for the WTI returns volatility since fluctuations of oil prices have a direct impact on the price of all goods and services that are produced using this source of energy. The estimated fractional differencing parameter equals 0.16, with an asymptotic standard error of 0.04, indicating significant long-memory component in the stock market volatility. So, a part of the persistence in the daily S&P 500 volatility may be modeled by the traditional *FIGARCH* and the rest can thus be attributed to the slow-variation of the baseline volatility. As for the WTI returns, an *AR*(3)-*TV-FIGARCH*(1,d,1,2) is

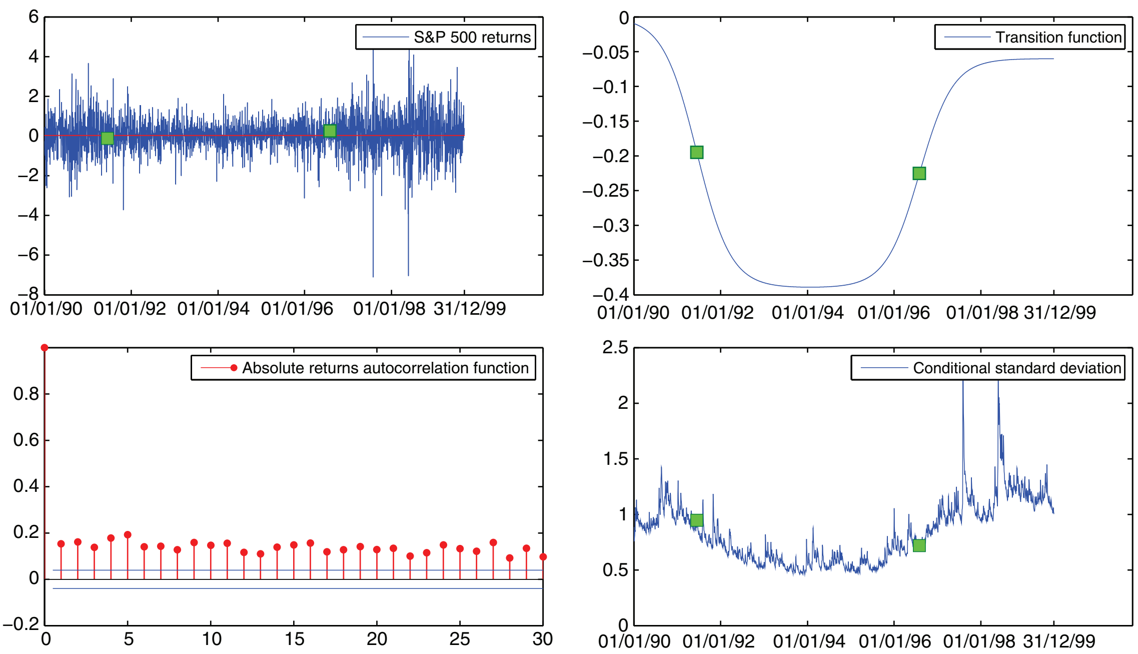

Fig. 4. Plots of the S&P 500 returns, the absolute returns autocorrelation function, the transition function f_t and the conditional standard deviations.

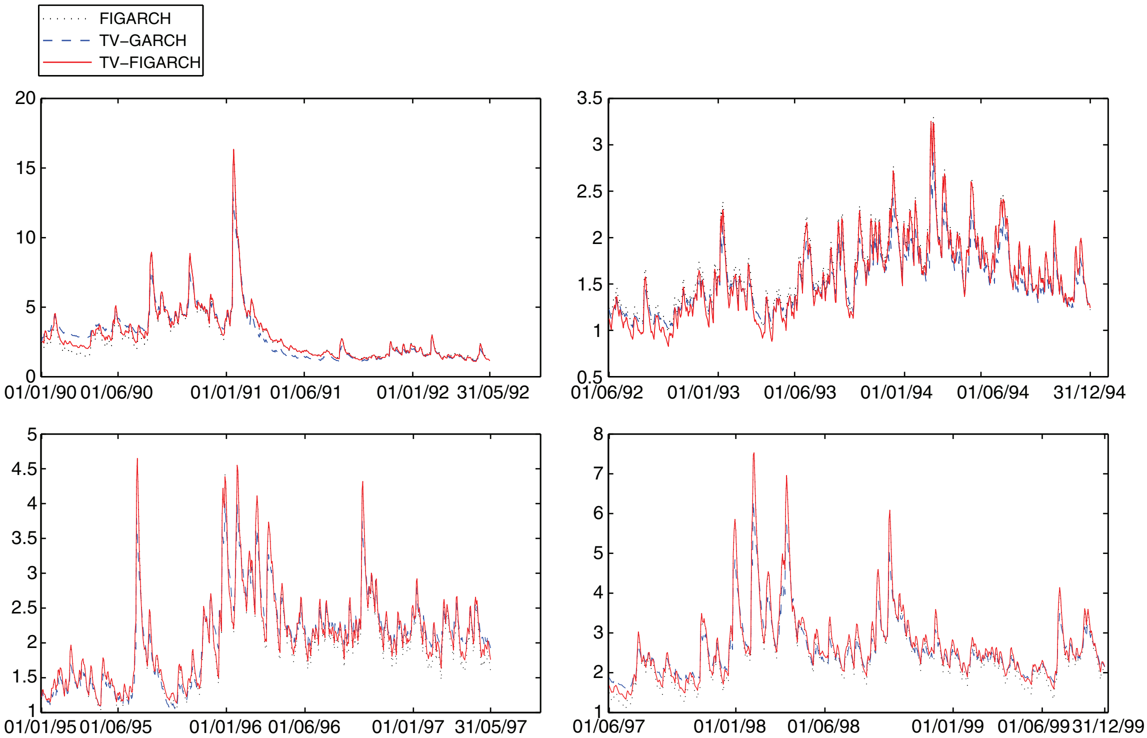

Fig. 5. Estimated conditional standard deviation from the FIGARCH (1, d, 1), the TV-GARCH (1, d, 1, 2) and the TV-FIGARCH (1, d, 1, 2) models for the WTI returns.

accepted as the final model for the S&P 500 returns (see Table 12). Table 13 contains the diagnostic test results and we notice that the skewness remains negative but the kurtosis coefficient shows some decrease. Relying on the Ljung-Box test and the ARCH test, the hypothesis of uncorrelated standardized and squared standardized residuals is well supported, indicating that there is no statistically significant evidence of misspecification. Though the significant decrease in the Jarque-Bera statistic, the standardized residuals are still not normally distributed.

6.3. Comparison between FIGARCH, TV-GARCH and TV-FIGARCH models

As the long memory and structural breaks are features which can be easily confounded, we provide in this section some estimations

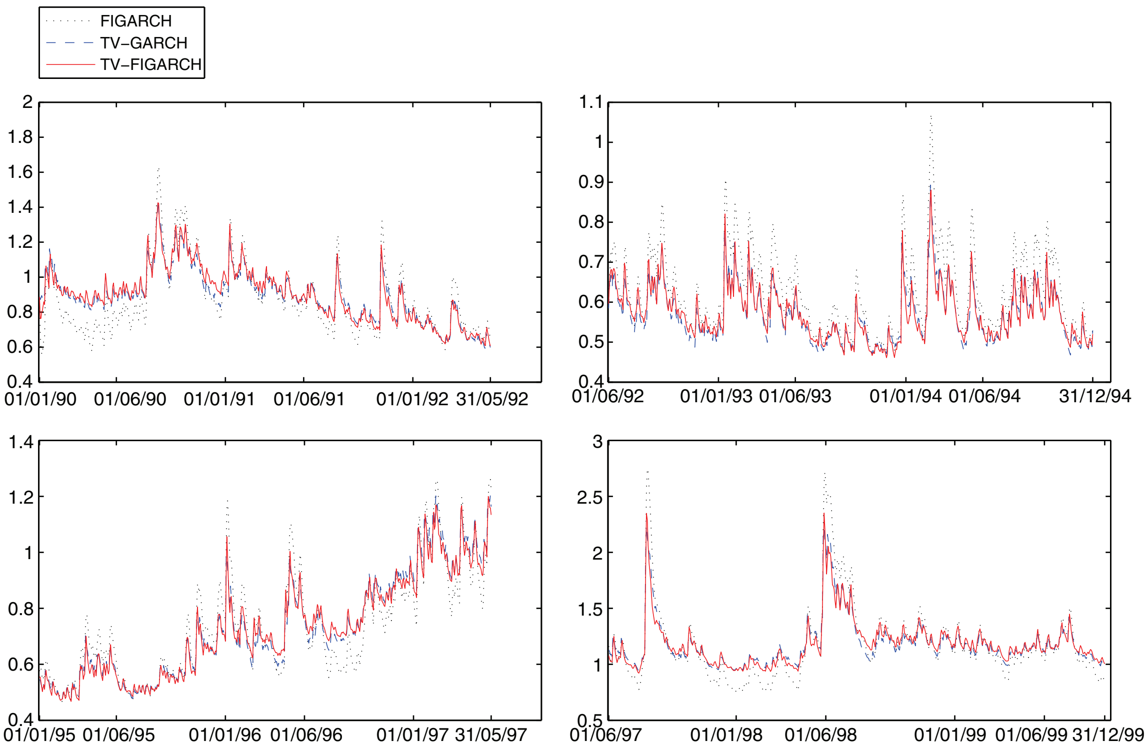

Fig. 6. Estimated conditional standard deviation from the FIGARCH (1, d, 1), the TV-GARCH (1, d, 1, 2) and the TV-FIGARCH (1, d, 1, 2) models for the S&P 500 returns.

between *FIGARCH*, *TV-GARCH* and *TV-FIGARCH* models, and some diagnostic test results.

For the *TV-GARCH* model, the constancy of the unconditional variance was also examined by means of the LM test described in Section 3. The results are not shown here, but the sequential testing procedure is carried out and a *TV-GARCH* model with two transitions is tentatively accepted as the final model. Teräsvirta and Amado (2008), who use the same data set of S&P 500 as in our application, select also a *TV-GARCH* model with two transitions for the volatility, but our transition function and theirs have different structures. From Table 12, we can see that estimates of the mean equation parameters are not statistically different across models. On comparison of the estimates of variance equation parameters, it can be seen that the *TV-FIGARCH* model corrects the upward bias in the autoregressive parameter of the *TV-GARCH* model, and reduces the estimated persistence parameter of the *FIGARCH* model. For both applications and for the *TV-GARCH* and the *TV-FIGARCH* models, the negative sign of $\hat{\omega}_1$ and the positive sign of $\hat{\omega}_2$ illustrate how volatility first decreases and then increases over time. However, we notice an increase in the smoothness parameter estimates of the *TV-GARCH* model and a slight difference in threshold parameter estimates between the two time-varying models. The performance of these models can be seen from their log likelihood function values as well as the Akaike and Schwarz (or Bayesian) information criteria values. We notice that the *TV-FIGARCH* model has the highest log likelihood function values and lowest AIC and SIC values, which indicates it may be the model with the best performance.

On comparison of the diagnostic tests results, the values of Ljung-Box statistics in the Table 13 show that the three models do a good job at capturing serial correlations in the standardized residuals, while the *TV-FIGARCH* model outperforms slightly the other models in eliminating serial dependence in the squared standardized residuals. We notice also that the highest p-value of the ARCH test and the lowest statistics of the Jarque-Bera normality test are for the *TV-FIGARCH* model. So, among the three models, the *TV-FIGARCH* model leads the others.

To obtain a clearer perception of the difference between the three models, the estimated conditional standard deviation from the *FIGARCH* (1,d,1), the *TV-GARCH*(1,d,1,2) and the *TV-FIGARCH*(1,d,1,2) models for the WTI and the S&P 500 returns are plotted in Figs. 5 and 6 respectively. As we can note from these plots, due to neglecting the unconditional variance changes over time, the estimated conditional standard deviation process from the *FIGARCH* model can show a significant bias, both upward and downward, relatively to the ones obtained by the *TV-GARCH* and the *TV-FIGARCH* models which look more synchronized.

7. Conclusion

This paper has proposed the *time-varying FIGARCH* or *TV-FIGARCH* process to model the volatility. This new flexible model has the feature to account for long memory and structural changes in the conditional variance whose intercept is allowed to be time-dependent. We also implement a modeling strategy for our *TV-FIGARCH* specification. To select the appropriate number of transitions, we use the Lagrange multiplier test on a sequence of hypothesis describing various dynamics of the baseline volatility over time. Our simulation experiments suggest that the parameter constancy tests have reasonable good properties and the modeling strategy appears to work quite well for the data-generating processes that we simulated. An empirical application to the crude oil price and the S&P 500 index are also included to illustrate the usefulness of our techniques. We find that the parameter constancy hypothesis is strongly rejected for both returns which may be linked to the Gulf War (1990–1991) and the economic boom in the United States and Asia in the mid-1990s followed by the financial crisis in the latter. Another empirical finding is that the long memory parameter estimates are statistically significant for both returns. Comparing our model to the *FIGARCH* and *TV-GARCH* models, our findings show that the long-memory type behavior of the sample autocorrelation function of the absolute returns is better modeled by a process which accounts for the time-variation in unconditional variance and the long memory in volatility. As conclusion, the autocorrelation function behavior of the absolute returns is not only induced by the presence of long memory in volatility, but also by structural breaks in the baseline volatility.

Appendix 1. Simulation results

Appendix 1.1. Size and power tests

Table 1
Simulated size for the test of *FIGARCH* (1, d, 1, 1) against the alternative *TV-FIGARCH* (1, d, 1, 1).

				α	1%	5%	10%
T	d	β	ϕ				
	0.25	0.20	0.60		0.08	0.17	0.17
1000	0.50	0.30	0.30		0.10	0.18	0.22
	0.75	0.60	0.20		0.10	0.20	0.24
	0.25	0.20	0.60		0.06	0.11	0.16
2000	0.50	0.30	0.30		0.09	0.15	0.18
	0.75	0.60	0.20		0.09	0.18	0.20
	0.25	0.20	0.60		0.06	0.09	0.11
3000	0.50	0.30	0.30		0.08	0.11	0.15
	0.75	0.60	0.20		0.09	0.15	0.18

Notes: Table 1 reports the rejection frequencies of the size test at the three theoretical significance levels {1%, 5%, and 10%}. The data generating process is given by DGP (I).

Table 2
Simulated power for the test of *FIGARCH* (1, d, and 1) against the alternative *TV-FIGARCH* (1, d, 1, and 1).

				α	1%	5%	10%
T	d	β	ϕ				
	0.25	0.20	0.60		0.66	0.81	0.87
1000	0.50	0.30	0.30		0.43	0.59	0.74
	0.75	0.60	0.20		0.36	0.53	0.73
	0.25	0.20	0.60		0.86	0.94	0.96
2000	0.50	0.30	0.30		0.68	0.75	0.85
	0.75	0.60	0.20		0.58	0.65	0.81
	0.25	0.20	0.60		0.89	0.93	0.98
3000	0.50	0.30	0.30		0.74	0.81	0.90
	0.75	0.60	0.20		0.70	0.77	0.85

Notes: Table 2 reports the rejection frequencies of the power test at the three theoretical significance levels {1%, 5%, 10%}. The data generating process is given by DGP (II).

Appendix 1.2. Model selection frequencies

Table 3
Model selection frequencies for the DGP (I).

				T	1000	2000	3000
d	β	ϕ	R				
			0		0.84	0.85	0.90
0.25	0.20	0.60	1		0.10	0.10	0.08
			2		0.06	0.05	0.02
			0		0.81	0.83	0.89
0.50	0.30	0.30	1		0.17	0.15	0.08
			2		0.02	0.02	0.03
			0		0.79	0.80	0.85
0.75	0.60	0.20	1		0.19	0.16	0.12
			2		0.02	0.04	0.03

Notes: Selection frequencies of the standard LM parameter constancy test based on 100 replications. The nominal significance level equals 5%.

Table 4
Model selection frequencies for the DGP (II).

d	β	ϕ	R \ T	1000	2000	3000
			0	0.02	0.01	0.01
0.25	0.20	0.60	1	0.82	0.87	0.92
			2	0.16	0.12	0.07
			0	0.06	0.05	0.03
0.50	0.30	0.30	1	0.67	0.78	0.85
			2	0.27	0.17	0.12
			0	0.09	0.06	0.04
0.75	0.60	0.20	1	0.63	0.75	0.78
			2	0.28	0.19	0.18

Notes: Selection frequencies of the standard LM parameter constancy test based on 100 replications. The nominal significance level equals 5%.

Table 5
Model selection frequencies for the DGP (III).

d	β	ϕ	R \ T	1000	2000	3000
			0	0.20	0.12	0.05
0.25	0.20	0.60	1	0.08	0.04	0.02
			2	0.72	0.84	0.93
			0	0.18	0.11	0.06
0.50	0.30	0.30	1	0.13	0.12	0.09
			2	0.69	0.77	0.85
			0	0.20	0.18	0.13
0.75	0.60	0.20	1	0.16	0.08	0.09
			2	0.64	0.74	0.78

Notes: Selection frequencies of the standard LM parameter constancy test based on 100 replications. The nominal significance level equals 5%.

Appendix 1.3. Estimation results

Table 6
Simulation on results estimating the *FIGARCH* (1, d, 1) model.

	$\hat{d}$	$\hat{\omega}_0$	$\hat{\beta}$	$\hat{\phi}$
True	0.25	0.50	0.20	0.60
Mean	0.30	0.55	0.22	0.59
RMSE	0.11	0.11	0.06	0.06
SE	0.02	0.03	0.02	0.02
True	0.50	0.50	0.30	0.30
Mean	0.54	0.51	0.31	0.39
RMSE	0.07	0.31	0.30	0.29
SE	0.02	0.06	0.07	0.05
True	0.75	0.50	0.60	0.20
Mean	0.76	0.55	0.60	0.19
RMSE	0.07	0.16	0.07	0.06
SE	0.02	0.04	0.02	0.02

Note: Table 6 reports the true parameters values, the sample mean of the Quasi Maximum Likelihood Estimates (QMLE), the root mean square error (RMSE) and the average of the standard errors (SE) of the parameters estimates, based on 100 replications and a sample size of T = 3000.

Table 7
Simulation results of estimating the *TV-FIGARCH* (1, d, 1, 1).

	$\hat{d}$	$\hat{\omega}_0$	$\hat{\beta}$	$\hat{\phi}$	$\hat{\omega}_1$	$\hat{\gamma}_1$	$\hat{c}_1$
True	0.25	0.50	0.20	0.60	−0.30	10	0.50
Mean	0.23	0.93	0.19	0.61	−0.58	63.46	0.45
RMSE	0.08	0.75	0.05	0.05	0.98	40.14	0.31
SE	0.02	0.56	0.01	0.01	1.93	100.36	0.82
True	0.50	0.50	0.30	0.30	−0.30	10	0.50
Mean	0.51	1.06	0.34	0.33	−0.09	65.04	0.44
RMSE	0.09	1.36	0.28	0.28	1.57	41.35	0.32
SE	0.02	1.09	0.08	0.08	2.30	121.16	0.62
True	0.75	0.50	0.60	0.20	−0.30	10	0.50
Mean	0.76	0.82	0.59	0.18	−0.55	63.28	0.51
RMSE	0.08	0.76	0.08	0.06	2.27	43.82	0.32
SE	0.02	0.83	0.02	0.02	3.36	109.43	0.39

See footnote to Table 6.

Table 8
Simulation results of estimating the *TV-FIGARCH* (1, d, 1, 2) model.

	$\hat{d}$	$\hat{\omega}_0$	$\hat{\beta}$	$\hat{\phi}$	$\hat{\omega}_1$	$\hat{\gamma}_1$	$\hat{c}_1$	$\hat{\omega}_2$	$\hat{\gamma}_2$	$\hat{\gamma}_2$
True	0.25	0.50	0.20	0.60	−0.30	10	0.30	0.30	10	0.70
Mean	0.22	1.27	0.18	0.60	−0.89	36.31	0.19	0.23	56.74	0.67
RMSE	0.08	0.98	0.06	0.05	1.42	38.33	0.17	0.91	42.13	0.23
SE	0.02	1.10	0.01	0.01	5.44	29.79	0.29	4.77	81.89	0.11
True	0.50	0.50	0.30	0.30	−0.30	10	0.30	0.30	10	0.70
Mean	0.53	1.26	0.42	0.41	−0.73	52.27	0.23	0.21	68.73	0.68
RMSE	0.09	1.59	0.29	0.30	2.28	41.41	0.19	1.86	41.60	0.23
SE	0.12	0.91	0.22	0.11	3.34	19.72	0.21	2.27	51.83	0.13
True	0.75	0.50	0.60	0.20	−0.30	10	0.30	0.30	10	0.70
Mean	0.79	1.28	0.61	0.18	−0.73	58.19	0.26	0.48	55.30	0.69
RMSE	0.09	1.66	0.08	0.09	2.43	41.44	0.19	1.98	42.62	0.22
SE	0.11	1.15	0.11	0.11	3.35	39.65	0.23	2.56	43.64	0.23

See footnote to Table 6.

Appendix 2. Empirical results

Table 9
Unit root test on the WTI and the S&P 500 returns.

	Intercept			Intercept and trend			
	ADF	PP	KPSS	ADF	PP	KPSS	Lags
WTI	−14.79	−56.46	0.07	−16.19	−56.47	0.04	12
S&P 500	−14.88	−50.39	0.32	−16.35	−50.46	0.02	10

Notes: the null hypothesis for ADF and PP tests is non stationarity, while it is stationarity for the KPSS test. The lag selection is based on the lowest AIC information criteria. The critical value for both the ADF and PP are −3.43, −2.86 and −2.51 and for the KPSS are 0.34, 0.46 and 0.73 at 1%, 5% and 10% levels of significance respectively for the model with intercept. The critical value for both the ADF and PP are −2.32, −1.64 and −1.28 and for the KPSS are 0.12, 0.14 and 0.21 at 1%, 5% and 10% levels of significance respectively for the model with intercept and trend.

Table 10
Summary statistics.

	WTI	S&P 500
Minimum	−40.63	−7.11
Maximum	18.86	4.98
μ	0.004	0.05
σ	2.52	0.88
sk	−1.63	−0.38
k	31.90	5.25
JB	10843 [0.00]	2958.8 [0.00]
Q(10)	87.55 $\left[1.63\ 10^{-14}\right]$	28.93 [0.0013]
Q(50)	243.00 [0.00]	79.33 [0.0048]
$Q^2(10)$	137.95 [0.00]	407.85 [0.00]
$Q^2(50)$	242.31 [0.00]	853.73 [0.00]
ARCH(4)	87.19 [0.00]	160.26 [0.00]

Notes: μ denotes the average returns and σ its standard deviation. *sk* is the Skewness coefficient, *k* is the Kurtosis and *JB* is the Jarque-Bera normality test, $Q(10)$, $Q(50)$, $Q^2(10)$ and $Q^2(50)$ are respectively the 10-th and 50-th orders Ljung-Box tests for serial correlation in the returns and squared returns.

Table 11
Test for selecting *R* for the WTI and the S&P 500 returns.

	WTI	S&P 500
H_{01}	2.161 [0.141]	2.95 [0.085]
H_{02}	5.784 [0.016]	9.87 [0.001]
H_{03}	5.435 [0.020]	2.68 [0.101]
H_{04}	5.619 [0.018]	3.40 [0.065]
H_{05}	3.062 [0.080]	6.32 [0.011]

Notes: the numbers in brackets are the p-values.

Table 12
Estimation results for the WTI and the S&P 500 returns.

	WTI			S&P 500		
	FIGARCH	TV-GARCH	TV-FIGARCH	FIGARCH	TV-GARCH	TV-FIGARCH
$\hat{\mu}$	−0.02 [0.02]	−0.01 [0.04]	−0.01 [0.03]	0.06 [0.005]	0.06 [0.003]	0.06 [0.004]
$\hat{\pi}_1$	0.02 [0.02]	0.01 [0.02]	0.02 [0.02]	0.05 [0.01]	0.05 [0.01]	0.05 [0.01]
$\hat{\pi}_2$	−0.04 [0.02]	−0.04 [0.02]	−0.03 [0.02]	0.03 [0.01]	0.02 [0.01]	0.01 [0.01]
$\hat{\pi}_3$	−0.09 [0.02]	−0.08 [0.02]	−0.09 [0.02]	−0.06 [0.01]	−0.06 [0.004]	−0.06 [0.01]
$\hat{d}$	0.63 [0.05]	-	0.57 0.056	0.43 [0.16]	–	0.16 [0.04]
$\hat{\omega}_0$	0.19 [0.46]	0.96 0.29	1.37 [0.54]	0.04 [0.03]	0.07 [0.05]	0.45 [0.23]
$\hat{\beta}$	0.56 [0.06]	0.86 [0.02]	0.50 [0.06]	0.54 [0.24]	0.78 [0.05]	0.17 [0.29]
$\hat{\phi}$	0.05 [0.04]	0.10 [0.02]	0.05 [0.06]	0.16 [0.14]	0.06 [0.03]	0.05 [0.27]
$\hat{\omega}_1$	–	−0.85 [0.27]	−1.31 [0.58]	–	−0.04 [0.04]	−0.39 [0.19]
$\hat{\gamma}_1$	–	176.32 [152.72]	106.14 [55.57]	–	39.86 [67.18]	24.67 [13.96]
$\hat{c}_1$	–	0.11 [0.02]	0.11 [0.01]	–	0.20 [0.04]	0.15 [0.04]
$\hat{\omega}_2$	–	0.20 [0.006]	0.57 [0.25]	–	0.07 [0.04]	0.33 [0.16]
$\hat{\gamma}_2$	–	189.76 [124.67]	8.15 [4.93]	–	27.09 [10.29]	24.97 [9.03]
$\hat{c}_2$	–	0.60 [0.14]	0.58 [0.14]	–	0.71 [0.02]	0.68 [0.03]
$log\ L(\lambda)$	−5439.14	−5419.96	−5414.24	−3027.56	−3005.96	−3000.25
AIC	10,896.28	10,865.92	10,856.48	6071.12	6037.92	6028.50
SIC	10,940.92	10,941.79	10,938.10	6117.76	6113.71	6110.12

Notes: table 12 reports QML parameter estimates of the AR(3)-FIGARCH(1,d,1), AR(3)-TVGARCH(1,d,1,2) and AR(3)-TVFIGARCH(1,d,1,2) models. $logL(\lambda)$ denotes the maximum value of the log likelihood function, AIC and SIC are the Akaike and Schwarz (or Bayesian) information criteria, respectively. The numbers in brackets are the robust standard errors.

Table 13
Diagnostic test results.

	WTI			S&P 500		
	FIGARCH	TV-GARCH	TV-FIGARCH	FIGARCH	TV-GARCH	TV-FIGARCH
sk	−0.29	−0.34	−0.27	−0.42	−0.39	−0.38
k	6.44	6.82	5.36	5.14	5.03	4.95
JB	1289.5 [0.00]	1589.60 [0.00]	617.86 [0.00]	559.37 [0.00]	499.76 [0.00]	466.58 [0.00]
$Q(10)$	5.11 [0.88]	3.26 [0.97]	4.00 [0.94]	10.54 [0.39]	10.07 [0.43]	9.41 [0.49]
$Q(50)$	36.89 [0.91]	38.84 [0.87]	40.07 [0.84]	66.59 [0.06]	63.57 [0.09]	63.43 [0.09]
$Q^2(10)$	8.91 [0.54]	11.86 [0.29]	8.44 [0.58]	5.06 [0.88]	4.47 [0.92]	4.36 [0.92]
$Q^2(50)$	47.48 [0.57]	41.07 [0.81]	40.47 [0.82]	42.34 [0.77]	39.86 [0.84]	38.88 [0.87]
ARCH(4)	1.75 [0.78]	5.10 [0.27]	1.58 [0.81]	2.98 [0.56]	2.26 [0.68]	2.14 [0.70]

Notes: sk is the Skewness coefficient, k is the Kurtosis and JB is the Jarque-Bera normality test. $Q(10)$, $Q(50)$, $Q^2(10)$ and $Q^2(50)$ are respectively the 10-th and 50-th orders Ljung-Box tests for serial correlation in the standardized and squared standardized residuals. The numbers in brackets are the p-values.

References

Baillie, R.T., Morana, C., 2009. Modeling long memory and structural breaks in conditional variances: an adaptive FIGARCH approach. Journal of Economic Dynamics & Control 33 (2009), 1577–1592.
Baillie, R.T., Bollerslev, T., Mikkelsen, H.O., 1996. Fractionally integrated generalized autoregressive conditional heteroskedasticity. Journal of Econometrics 74, 3–30.
Beine, M., Laurent, S., 2000. "Structural change and long memory in volatility: new evidence from daily exchange rates". *working paper, University of Liege*.
Beltratti, A., Morana, C., 2006. Breaks and persistency: macroeconomic causes of stock market volatility. Journal of Econometrics 131, 151–171.
Beran, J., Ocker, D., 1999. "Volatility of stock market indices-an analysis based on SEMIFAR models". *mimeo, University of Kostanz*.
Boes, D.C., Salas-La Cruz, J.D., 1978. Non stationarity of the mean and the Hurst phenomenon. Water Resources Research 14, 135–143.
Bollerslev, T., 1986. Generalized autoregressive conditional heteroskedasticity. Journal of Econometrics 31, 307–327.
Bollerslev, T., Mikkelsen, H.O., 1996. Modeling and pricing long memory in stock market volatility. Journal of Econometrics 73, 151–184.
Conrad, C., Haag, B.R., 2006. Inequality constraints in the fractionally integrated GARCH model. Journal of Financial Econometrics 4 (3), 413–449.
Dahlhaus, R., Subba Rao, S., 2006. Statistical inference for time-varying ARCH processes. Annals of Statistics 34, 1075–1114.
Diebold, F.X., Inoue, A., 1999. "Long memory and structural change". *Stern School of Business discussion paper*.
Eitrheim, Ø., Teräsvirta, T., 1996. Testing the adequacy of smooth transition autoregressive models. Journal of Econometrics 74, 59–75.
Engle, R.F., 1982. Autoregressive conditional heteroscedasticity with estimates of the variance of United Kingdom inflation. Econometrica 50, 987–1007.
Engle, R.F., Rangel, J.G., 2005. The Spline GARCH model for unconditional volatility and its global macroeconomic causes: Czech National Banks Working Paper Series, 13.
Fong, W.M., See, K.H., 2002. A Markov switching model of the conditional volatility of crude oil futures prices. Energy Economics 24, 71–95.
Gallant, A.R., 1984. The fourier flexible form. American Journal of Agricultural Economics 66, 204–208.
Gourieroux, C., Jasiak, J., 2001. Memory and infrequent breaks. Economics Letters 70, 29–41.
Granger, C.W.J., Hyung, N., 1999. Occasional structural breaks and long memory. UCSD discussion paper 99-14.
Granger, C.W.J., Hyung, N., 2004. Occasional structural breaks and long memory with an application to the S&P500 absolute returns. Journal of Empirical Finance 11 (3), 399–421.
Hamilton, J., Susmel, R., 1994. Autoregresive conditional heteroskedasticity and changes in regime. Journal of Econometrics 64, 307–333.
Hosking, J.R.M., 1981. Fractional differencing. Biometrika 68, 165–176.
Kwiatkowski, D., Phillips, P.C.B., Schmidt, P., Shin, Y., 1992. Testing the null hypothesis of stationarity against the alternative of a unit root: how sure are we that economic time series have a unit root? Journal of Econometrics 54, 159–178.
Lobato, I.N., Savin, N.E., 1998. Real and spurious long memory properties of stock market data. Journal of Business and Economic Statistics 16 (3), 261–268.
Lundbergh, S., Teräsvirta, T., 2002. Evaluating GARCH models. Journal of Econometrics 110, 417–435.
Luukkonen, R., Saikkonen, P., Teräsvirta, T., 1988. Testing linearity against smooth transition autoregressive models. Biometrika 75, 491–499.
Martens, M., van Dijk, D., de Pooter, M., 2004. "Modeling and Forecasting S&P 500 Volatility: Long Memory, Structural Breaks and Nonlinearity": *Tinbergen Institute Discussion Paper*. 04-067/4.
Morana, C., Beltratti, A., 2004. Structural change and long range dependence in volatility of exchange rates: either, neither or both? Journal of Empirical Finance 11, 629–658.
Phillips, P.C.B., Perron, P., 1988. Testing for a unit root in time series regression. Biometrika 75, 335–346.
Said, E.S., Dickey, A.D., 1984. Testing for unit roots in autoregressive-moving average models of unknown order. Biometrika 71 (3), 599–607.
Schwert, G.W., 1989. Business cycles, financial crises, and stock volatility? Carnegie-Rochester Conference Series on Public Policy 31, 83–126.
Starica, C., Granger, C., 2004. "Non-Stationarities in Stock Returns". *working paper, University of California San Diego*.
Teräsvirta, T., Amado, C., 2008. Modelling conditional and unconditional heteroscedasticity with smoothly time-varying Structure. Stockholm School of Economics SSE/EFI, Working Paper Series in Economics and Finance No. 691.
Wilson, B., Aggarwal, R., Inclan, C., 1996. Detecting volatility changes across the oil sector. Journal of Futures Markets 16, 313–320.